



NEW ZEALAND SOCIETY FOR EARTHQUAKE ENGINEERING
**2019 Pacific Conference on
Earthquake Engineering**
TURNING HAZARD AWARENESS INTO RISK MITIGATION
4 – 6 April | SkyCity, Auckland | New Zealand



Damage-avoidance timber brace using a self-centring friction damper

S.M.M. Yousef-beik & P. Zarnani

Auckland University of Technology, New Zealand, Auckland.

H. Bagheri, A. Hashemi & P. Quenneville

University of Auckland, New Zealand, Auckland.

ABSTRACT

Self-centring systems are gaining more popularity among engineers as ductile and reliable seismic resistant systems due to their repeatable, reusable and adjustable cyclic behaviour. Usage of timber as a structural member in multi-storey structures is also acquiring more demand owing to advantages that this material can bring such as aesthetic considerations, lower environmental footprint, the speed of fabrication and high strength to weight ratio. This paper attempts to develop and experimentally verify a new damage-avoidance self-centring timber brace which can provide energy dissipation and self-centring characteristics while it does not have the concerns regarding the conventional timber braces such as pinched hysteretic response, strength degradation and stiffness degradation. Furthermore, a comparative study for a prototype four-storey building equipped with the proposed brace and Buckling-restrained Brace (BRB), one of the most efficient and commonly used steel braces, is conducted with the intention of further clarification on the performance of this novel bracing system.

1 INTRODUCTION

Concentrically Timber Braced Frames (CTBFs) are efficient lateral load resisting systems, which can deliver suitable elastic (initial) stiffness in case of low and moderate seismic attacks, relying on the stiff behaviour of the timber when being loaded parallel to grain. However, the application of timber braces or timber structures in regions with high seismic activity is of concern as the ductility and energy dissipation capacity for these buildings is provided only by steel connections and not timber due to its brittle behaviour (Popovski al.2003). Due to this, most of the current building codes such as ASCE 7 normally assumes relatively lower force reduction factors for timber structures as compared to either steel or concrete structures and will not allow for construction in regions with a high-seismic activity (Category E and F). As a result, the literature associated with the timber braces is noticeably less as compared to that of steel braces. Based on the type of

connection and steel connectors which is used for a timber brace, the behaviour and ductility of the system may change (Popovski, 2000). (Popovski et al. 2008) studied and tested CTBFs with timber riveted connections. During their tests, the following observations were made: Firstly, the cyclic behaviour of the brace (hysteric curves) were severely pinched (Popovski et al, 2008) which is a common phenomenon in the timber connections and lies in the irreversible timber crushing. The second observation was the strength degradation, which is of two types: in-cycle degradation happening within a cycle and cyclic strength degradation happening through a number of inelastic cycles (FEMA p440). Both were observed in the experiments. Although there was no report on the residual drift of the timber brace in that study, residual displacement does matter when the economic losses such as cost for realignment and repair, business interruption and so on are taken into account (Ramirez et al. 2012). Another problem regarding the residual drift is that it makes the building vulnerable to aftershock events. A recent study (Veismoradi et al.2018) shows that if the aftershock events are considered, a type of structures are 50% more probable to collapse.

In this paper, a new Timber brace-type lateral load resisting system with respect to Damage Avoidance Design (DAD) (Rodgers et al. 2015) will be proposed and experimentally verified by adopting the newly developed Resilient Slip Friction Joints entitled “RSFJs” (Zarnani & Quenneville, 2015). Generally, there are three main objectives to be met when designing in accordance with DAD. The first and foremost one is that system should not allow any damage when subjected to both gravity and lateral load resisting system. The second one is that there should be some recentring capability so that the structure would be realigned and ready to be re-occupied after experiencing a major earthquake. Last is that a DAD system should have a repeatable, reliable and reusable damping mechanism. In this regard, the proposed bracing system is expected to meet all above-mentioned criteria while importantly it does not have the concerns regarding the conventional timber brace – pinching, strength degradation and residual displacement. It should be noted that this brace can be employed for steel, concrete and timber structures.

2 AXIAL PERFORMANCE OF THE RSFJ

As it is shown in Figure 1 (a), the RSFJ damper is composed of two kinds of steel plate namely: cap plates and middle plates. These plates are clamped together by means of high strength bolts and disc springs through their grooved surface. The flag-shape performance of RSFJ is depicted in Figure 1 (b). In this diagram, slip force is indicative of the force at which joint will start to move also meaning that the prestressing force of disc springs is overcome. After the slip point, the axial displacement of the joint in the loading process will be mapped into a vertical displacement (depending on the angle of grooves), resulting in more compaction of disc springs and can be continued until the discs are fully flat. On the contrary, when the stored energy in the disc springs is being released within the unloading phase, the frictional resistance will be reversed in direction. This change in the friction direction provides the required damping during the cyclic loading and will form the flag-shape response for the RSFJ (Fig.1 (b)). The slip force of RSFJ can be calculated by (Hashemi et al., 2019):

$$F_{slip} = 2n_b F_{b,pr} \left(\frac{\sin(\theta_g) + \mu \cos(\theta_g)}{\cos(\theta_g) - \mu \sin(\theta_g)} \right) \quad (1)$$

Where, “ θ_g ” denotes the angle of grooves; “ μ_k ” is the coefficient of kinetic friction and can be assumed as $0.85 \mu_s$ (coefficient of static friction). “ $F_{b,pr}$ ” indicates the bolt force due to prestressing of disk springs; and “ n_b ” is the number of bolts on each splice (For instance, in Figure 1, n_b equals 2). Similarly, the residual force at the end of unloading can be calculated by Equation (2):

$$F_{res} = 2n_b F_{b,pr} \left(\frac{\sin(\theta_g) + \mu \cos(\theta_g)}{\cos(\theta_g) - \mu \sin(\theta_g)} \right) \quad (2)$$

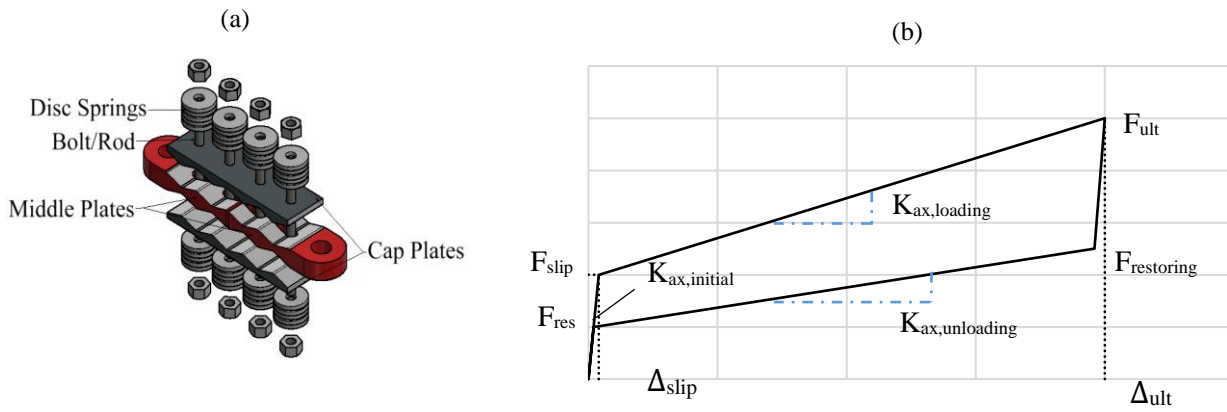


Figure 1: (a) RSF joint assembly and components, (b) Passive self-centring hysteretic axial response of RSFJ (flag-shaped hysteresis)

The maximum load that a joint can experience (F_{ult}) is when the disc springs are fully flat, so by replacing “ $F_{b,pr}$ ” by “ $F_{b,u}$ ” – which is the resultant force of the disc springs in a series in the fully flat position – in “ F_{slip} ” and “ F_{res} ”, the maximum load and restoring force will be yielded. For more information concerning the criteria required for self-centring and different types of the RSFJ, refer to (Hashemi et al. 2016; Yousef-beik et al. 2018; Zarnani et al. 2016). Regarding the slope of flag-shape for axial behaviour during loading, it can be simply calculated by the following equation:

$$K_{ax,loading} = n_b K_{st} \tan(\theta_g) \left(\frac{\sin(\theta_g) + \mu \cos(\theta_g)}{\cos(\theta_g) - \mu \sin(\theta_g)} \right) \quad (3)$$

Where “ K_{st} ” is the equivalent stiffness for the stack of springs. Similar procedure can be done for unloading phase with friction force in opposite direction resulting in:

$$K_{ax,unloading} = n_b K_{st} \tan(\theta_g) \left(\frac{\sin(\theta_g) - \mu \cos(\theta_g)}{\cos(\theta_g) + \mu \sin(\theta_g)} \right) \quad (4)$$

The interesting point regarding the slope of the flag-shape in loading and unloading is that both of them are only functions of characteristics of the stack of discs, the angle of grooves and the coefficient of friction. The percentage of restressing does not contribute in the slop of the flag-shape.

3 EXPERIMENTAL DEMONSTRATION OF THE BRACE BEHAVIOUR WITH REVERSED CYCLIC TESTS

A scaled timber brace was designed in accordance with DAD concept. In this concept, all the energy dissipation will be provided by the RSFJ damper, and the steel connections and the timber body should stay elastic during the whole loading. Considering a scale factor of 1/2.4, the tested brace with a length of 1701 mm can be the representative for a frame with 3.3-meter height and 5-meter length with a converse V-type bracing configuration. The brace specimen was made up of two main sections. One timber body and one RSFJ damper. The timber part was composed of an LVL grade 11 with an elastic modulus of $E = 11$ GPa and a density of $\rho = 500$ kg/m³. Besides, it had a 150 mm wide square-shape cross section. The timber body part had parallel to grain nominal tension and compression capacity of 740 kN and 910 kN, respectively (according to the Eurocode 5). There were two end bracket plates with a thickness of 20 mm with a pin hole in them to provide the pin ended situation for the brace (shown in Figure 2). The connection between the bearing plates and the timber column was capacity designed (with respect to capacity of damper) and a total number of 8 self-tapping screws with 180 mm length and 7 mm diameter were used for the attachment. An actuator with 300 kN force and 100 mm stroke capacity was utilized for this test. The schematic drawings of the brace and the test setup used are illustrated in Figure 2. For the purpose of data acquisition, two

displacement gauges were used at both sides of the RSFJ to measure the axial deformation of the specimen. Furthermore, two Linear Variable Differential Transformers (LVDTs) were employed along the height of the brace to record the lateral displacement. Different configurations including four different stacks with different number of springs and pre-stressing forces were considered for the testing program (see table 1). It should be noted that the stiffness associated with each stack - " K_{st} " for 5, 6, 8 and 11-disc springs - were 7.686 KN/mm, 6.405 KN/mm, 4.292 KN/mm and 4.73 KN/mm respectively.

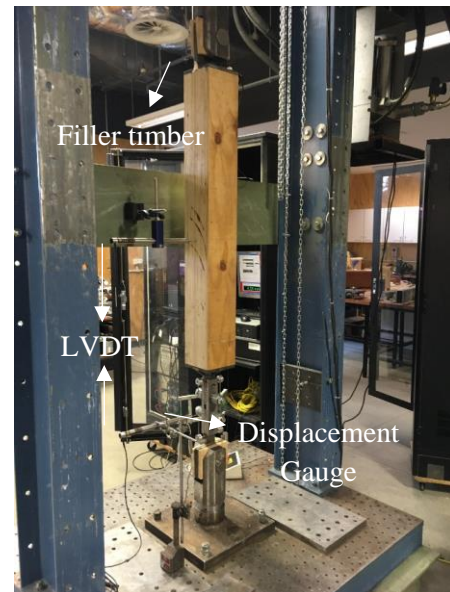


Figure 2: Test setup and specimen: (a) Side views of test specimen for the in-plane testing (b) Experimental test setup

The following reversed cyclic loading protocol shown in Figure 3 according to AISC (AISC, 2010) suggestion for BRB braces is used for this testing program. As it can be seen, the loading regime contains a maximum of 9 mm displacement that is indicative of almost 2% lateral drift. Note that in this study, the drift associated with DBE is assumed to be 1% while the drift associated with Maximum Considerable Earthquake (MCE) is assumed to be twice of the DBE drift which mean 2%. Displacement control approach was performed for the testing procedure.

Table 1: Different configurations for the RSFJ brace

Configuration	n_d	γ (%)	F_{slip} (KN)	$F_{sresidual}$ (KN)	F_{ult} (KN)	$F_{restoring}$ (KN)
1	5	18	11.3	4.07	38.9	17.4
2	6	13	7.9	3.85	30.9	15
3	8	13	7.9	3.85	23.7	11.5
4	11	40	24.3	11.85	40.7	19.8

The experimental results of the tested timber brace are illustrated in Figure 4. As it can be observed, the analytical envelope (red dotted lines) predicted with analytical formulas are in good agreement with the experimental results of the reversed cyclic test. As it can be concluded from figures, firstly, the loading and unloading post-slip stiffnesses are different, and secondly, they are adjustable with respect to the number of the disc springs used (refer to Equation 3 and Equation 4). More specifically, the loading and unloading post-slip stiffnesses are inversely proportional to the number disc springs. As an illustration, the configuration 4 with 11-disc springs ($n_d = 11$) had the lowest post-slip stiffness while configuration 1 possessed the highest post-slip stiffness.

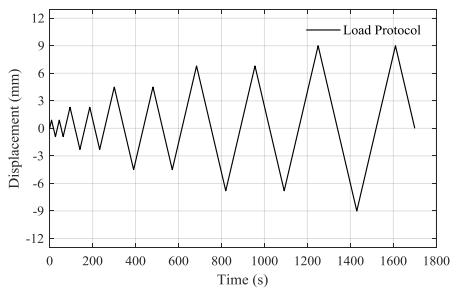


Figure 3: The loading protocol

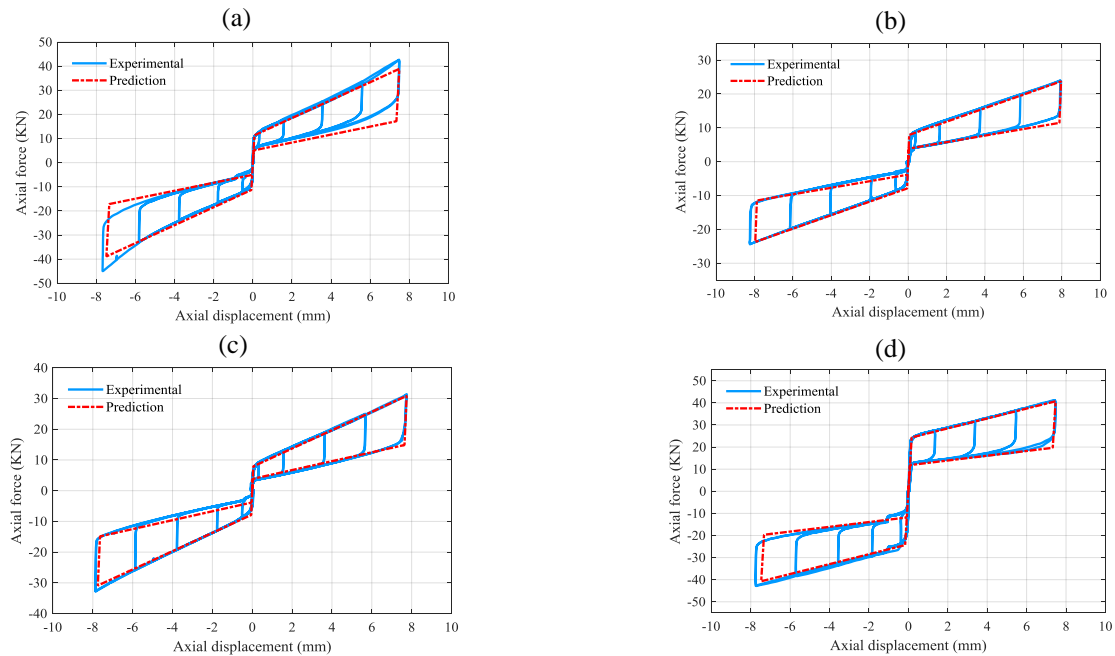


Figure 4: Test results: (a) flag-shape response of the configuration 1, (b) flag-shape response of the configuration 2, (c) flag-shape response of the configuration 3 and (d) flag-shape response of configuration 4.

4 COMPARATIVE STUDY ON SEISMIC PERFORMANCE OF A PROTOTYPE BUILDING WITH BRB BRACE AND RSFJ BRACE

A four-storey frame (shown in Figure 5), which was originally designed for study of BRB frames (Vafaei et al, is used here as a reference model to demonstrate the performance of the RSFJ brace system. For further information regarding the member sizes and BRB sections, refer to (Vafaei et al, 2015). The displacement ductility (shown in Figure .10(a) factor associated with the reference BRB building is assumed to be 2.5 in this study while it can be assumed even higher up to 3 ($\mu = 3$) according to (Wijanto, 2012) with respect to New Zealand Code NZS 1170. This displacement ductility factor will result in a force reduction factor (shown in Figure 9 (a)) of 2.1 with respect to the fundamental period of the structure according to NZS 1170. This building is assumed to be constructed in Christchurch, which is of high seismicity, on a soil type D (stiff soil) and with a distance of 5 Km from a major fault according to New Zealand Code NZS 1170 (NZS 1170.5, 2004) . It should be also noted that the codified design base shear for this building is matched with the base shear for the original building designed for Los Angeles city. In this respect, a suite of 10 ground motions were selected and scaled to Ultimate Limit State (ULS) earthquake with respect to New Zealand code. The associated target and mean spectrums are provided in Figure 6 (a).

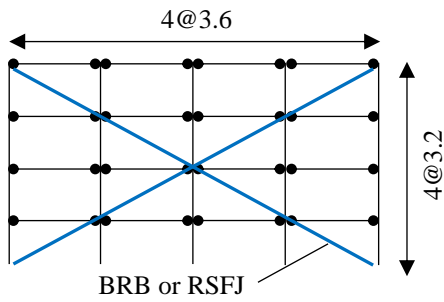


Figure 5: The Prototype four-storey Structure

Table 2: Selected ground motions for NTH

No.	Name	Magnitude	Year	Scale Factor
1	Chi Chi	7.62	1999	0.6
2	Christchurch	6.3	2011	1.65
3	Duzce	7.2	1999	0.67
4	Hokkaido	8.3	2003	0.89
5	Kaikoura	7.8	2016	1
6	Kobe	6.9	1995	0.85
7	Landers	7.28	1992	0.98
8	LomaPrieta	6.93	1989	0.93
9	Northridge	6.69	1994	0.61
10	Kocaeli	7.5	1999	0.78

Nonlinear Time History (NTH) analyses was conducted using the SAP2000 software in which plastic (Wen) hysteresis model was used with the intent of modelling the BRB brace behaviour. In order to verify the accuracy of the modelling method, a component BRB brace is simulated in SAP2000 software before modelling the building and was calibrated with the experimental results of specimen 99-1 from PEER Report 2002/8 (Black et al. 2002) using far-field load protocol. In that report, the BRB had a rectangular shaped steel core with ASTM A572/50 with yielding stress of 345 MPa. The result of calibration is shown in Figure 6 (b). The resulted calibration parameters including smoothness of edges and post-yield stiffness were then used for modelling the other braces. As it can be seen in Figure 6 (b), there is a good agreement between the calibrated numerical and experimental results.

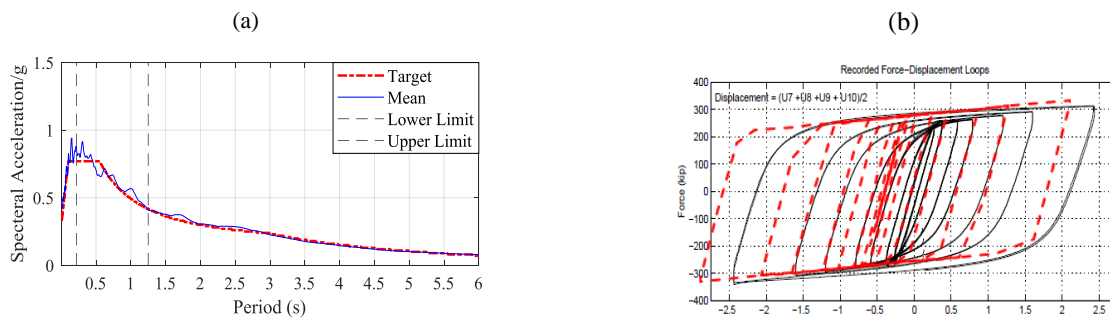


Figure 6: (a) Target and mean spectrum, (b) Calibration of a BRB component in the SAP2000 with experimental results (Black et al., 2002)

The precise modelling of the building is another parameter that had be taken into consideration. In this respect, the first three fundamental periods of the structure modelled in SAP2000 are compared to those of original work (Vafaei et al. 2015), which was performed within the OpenSees software package. The results of modal analysis are summarized in Table 3 based on which it can be seen that the periods are very close to each other. This demonstrates that the building is correctly modelled in SAP2000 software in terms of mass and stiffness.

Table 3: Comparison of First Three Periods

Period	Original building modelled in OpenSees (Vafaei et al 2015)	Numerical model with SAP2000 used in this paper
1	0.537 s	0.550 s
2	0.213 s	0.241 s
3	0.152 s	0.164 s

After verifying the model with BRB, the same four-storey building was used with the RSFJ brace in a way that both buildings reach relatively the same base shear at 2.5 % drift. In this process, the force and deflection capacity and initial stiffness of RSFJ braces were assumed to be approximately identical with those of BRB braces. The reason for these assumptions is to better compare the seismic performance of both buildings. With current assumptions, the deflection capacity and elastic behaviour of both buildings tends to be the same. The only thing that differs and importantly it is aimed to be studied is their inelastic behaviour and seismic demands. The design summary of BRB and RSFJ braces are provided in Table 4. It should be noted that as the design of RSFJ is flexible, these parameters can be really achieved in practice. In order to model the RSFJ brace in the SAP2000, the Damper - Friction-Spring link element (Hashemi et al. 2019), which provides a flag-shape hysteresis curve, was used.

Table 4: RSFJ and BRB Design summary for each storey

Story	BRB				RSFJ					
	Initial Stiffness (KN/mm)	F_y (KN)	F_u (KN)	Δ_u (mm)	Initial Stiffness (KN/mm)	F_{slip} (KN)	F_{ult} (KN)	F_{unload} (KN)	F_{res} (KN)	Δ_u (mm)
1	133767	847.67	1165.5	101	133767	639	1162	269	148	102
2	112670	713.98	981.7	101	112670	561	950.7	220.4	130	102
3	84479	535.34	736	101	84479	436	739	171.4	101	102
4	63251	401.65	552	101	63251	311	528	122.5	72	102

Figure 7 depicts the nonlinear static analysis or pushover analysis of the both buildings when they are subjected to a triangular load pattern. As it can be observed, the base shear at 2.5% drift associated with both buildings are almost equal. In the following, more details will be provided for seismic performance of both buildings.

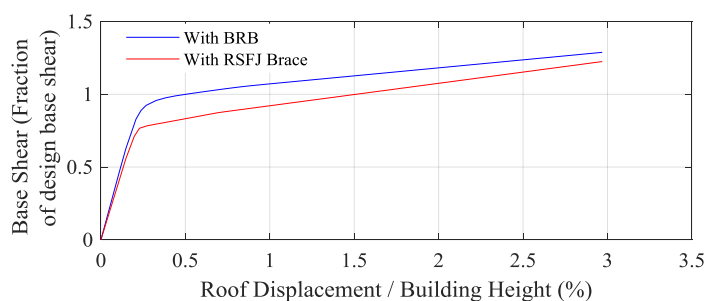


Figure 7: Cyclic Pushover results with amplitude of 2.5% drift

For the purpose of NTH analysis, 10 earthquakes were opted (shown in Table 2) from which 9 were scaled to match the elastic design spectrum of New Zealand code for ULS and one of them (Kaikoura) was applied without any scaling. The results of the NTH analysis are provided in Figure 8.

According to Figure 8 (a, b), all the maximum inter-storey drifts associated with both structures were less than 2.5% (the codified limitation for the inter-storey drift). It should be also noted that the mean storey drifts

associated with upper two floors (3rd and 4th floor) were almost equal for both buildings while it was higher for building with RSFJ brace for the first two stories.

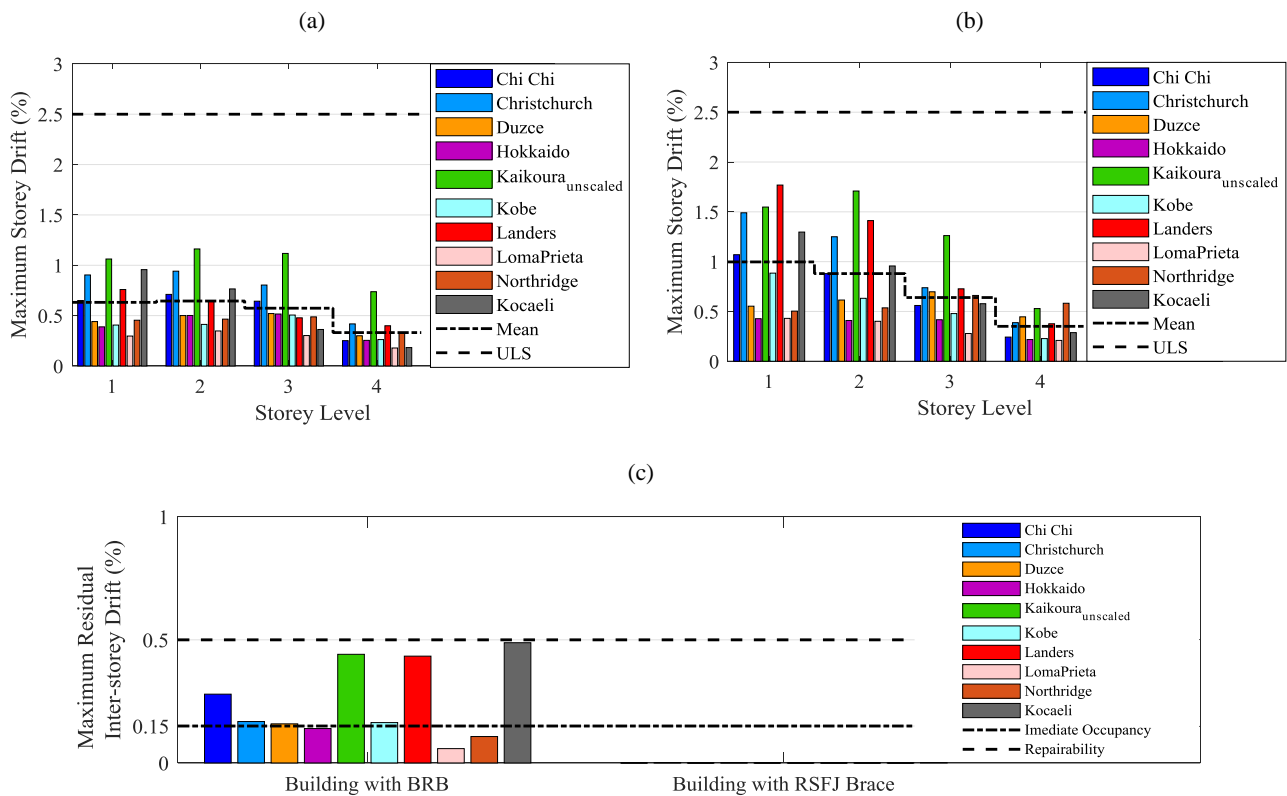


Figure 8: (a, b) Maximum inter-storey drift for building with BRB and RSFJ brace, (c) Maximum residual inter-storey drift.

Figure 8 (c) presents the maximum residual inter-storey drift for both structures. According to current practise of performance-based design, if the residual drift is less than a limit (normally between 0.1 – 0.2 % (Clifton et al. 2012; Erochko et al. 2010; Ghobarah et al. 2001)) herein is assumed to be 0.15 % after a major seismic attack, the building can be reoccupied immediately with no serviceability disruption and; therefore, it can be regarded as a low damage seismic resisting system. In another case, if the residual displacement is between 0.15 and 0.5%, it can be repaired and reused, yet the repair time and cost should be considered after the event. Lastly, if the residual drift exceeds 0.5%, the cost of demolishing and rebuilding would be less than repair (Erochko et al. 2010; Ghobarah, 2001). In this respect, for all of the events, the RSFJ building managed to keep the residual drift to the least possible (zero) so it can be reoccupied immediately. As the residual displacement is zero and all the materials are kept within their elastic zone, it can be classified as a DAD system. On the contrary, the BRB building was near to be regarded as non-repairable (Drift > 0.5 %) for three events, needed to be repaired for five events, and can be reoccupied immediately for two events. This results attempt to confirm the previous findings of scholars such as (Erochko et al., 2010; Veismoradi et al., 2018).

Figure 9 (a) describes the definition of force and displacement reduction factor (referred to as k_{μ} and μ in New Zealand code) resulting from comparing the elastic base shear with the reduced base shear due to nonlinear behaviour of the building. The nonlinear behaviour in BRB building was coming from the yielding and inelastic behaviour of the BRB brace while in building with RSFJ brace, it was coming from nonlinear elastic (flag-shape) behaviour of the slip-friction damper (RSFJ). The reduction factors for both buildings with RSFJ and BRB brace subjected to the input earthquakes are summarized in Figure 9 (b). As it can be seen, at most of the cases, the building with RSFJ brace showed higher force reduction capability or relatively lower base shear. More specifically, the mean force reduction factor for BRB was roughly 2 ($K_{\mu} = 2.07$) which confirms the initial assumptions of $K_{\mu} = 2.1$ while it was around 2.3 for RSFJ building. It

should be also noted that these presented results are for the low-rise building and not general, and further studies are required for the buildings with higher periods. The key characteristic that resulted in lower base shear for RSFJ brace building is its sooner activation than BRB. In fact, the activation point of RSFJ or slip point can be adjusted with prestressing force in the disc springs.

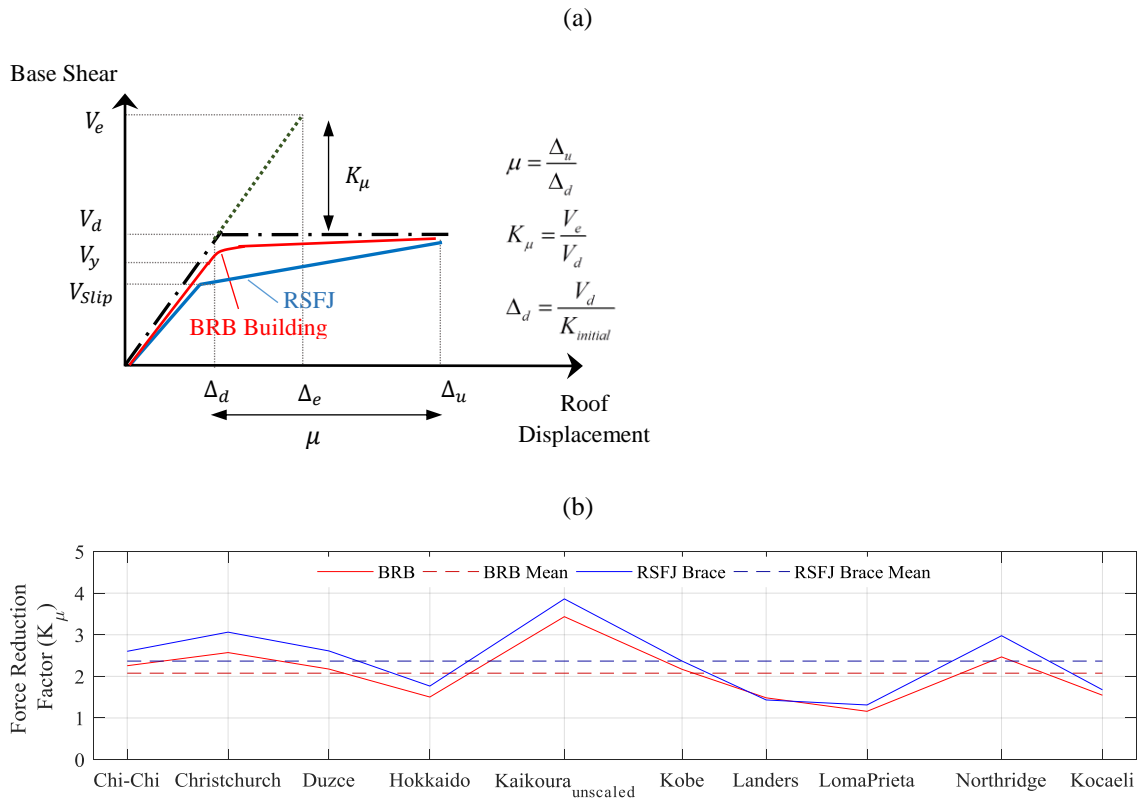


Figure 9: (a) Seismic reduction factors according NZ 1170, (b) Force reduction factor based on NTH results

5 CONCLUSION

This study presented a new damage avoidance self-centring timber brace which not only lacks the concerns associated with the conventional timber braces such as pinching, timber crushing and strength and stiffness degradation, but also possesses the strong points of new efficient braces such as BRB while it possess zero residual displacement. In the first part of this paper, an analytical model was developed to predict the response of both RSFJ damper and RSFJ brace. In the second part of this study, experimental validations were provided for the performance of the proposed brace in which four different brace configurations were experimentally tested. In the last part, the seismic performance of the building was studied using a reference BRB frame. According to this simulations, zero-residual drift was observed for the proposed brace. Besides, relatively higher maximum inter-storey responses were observed for the RSFJ brace, yet the design base shear was 15% less for the RSFJ building. Regarding the difference for inter-storey drift, it should be noted that it got smaller as the floor increased. The difference for the first floor was almost 50% while it was 5% for the level 4.

6 ACKNOWLEDGEMENT

The authors would like to thank the Earthquake Commission (EQC) of New Zealand and the Ministry of Business, Innovation and Employment of New Zealand (MBIE) for the financial support provided for this research. The commercial interest for Tectonus company manufacturing RSFJ damper is acknowledged.

7 REFERENCES

- NZS.5. 2004. *Structural Design Actions, Part 5: Earthquake Actions—New Zealand*: Standards New Zealand Wellington, New Zealand.
- AISC, A. 2010. *AISC 341-10, Seismic Provisions for Structural Steel Buildings*. Chicago, IL: American Institute of Steel Construction.
- Black, C., Aiken, I.D. & Makris, N. 2002. *Component testing, stability analysis, and characterization of buckling-restrained unbonded braces (TM)*: Pacific Earthquake Engineering Research Center.
- Clifton, G., Bruneau, M., MacRae, G., Leon, R. & Fussell, A. 2012. *Multistorey steel framed building damage from the Christchurch earthquake series of 2010/2011*, Behaviour of Steel Structures in Seismic Areas: STESSA 2012, 15.
- Erochko, J., Christopoulos, C., Tremblay, R. & Choi, H. 2010. Residual drift response of SMRFs and BRB frames in steel buildings designed according to ASCE 7-05, *Journal of Structural Engineering*, Vol 137(5) 589-599.
- FEMA, P. 440A. 2009. *Effects of strength and stiffness degradation on seismic response*, Federal Emergency Management Agency, Washington, DC.
- Ghobarah, A. 2001. Performance-based design in earthquake engineering: state of development, *Engineering structures*, Vol 23(8) 878-884.
- Hashemi, A., Yousef-Beik, S.M.M., Darani, F.M., Clifton, G.C., Zarnani, P. & Quenneville, P. 2019. Seismic performance of a damage avoidance self-centring brace with collapse prevention mechanism, *Journal of Constructional Steel Research*, Vol 155 273-285.
- Hashemi, A., Zarnani, P., Valadbeigi, A., Masoudnia, R. & Quenneville, P. 2016. Seismic resistant cross laminated timber structures using an innovative resilient friction damping system, *Proc. New Zeal. Soc. Earthq. Eng. Conf.(NZSEE)*, Christchurch, New Zealand
- Popovski, M. 2000. *Seismic performance of braced timber frames*. University of British Columbia.
- Popovski, M. & Karacabeyli, E. 2008. Force modification factors and capacity design procedures for braced timber frames, *14th World Conference on Earthquake Engineering (14WCEE)*
- Popovski, M., Prion, H.G. & Karacabeyli, E. 2003. Shake table tests on single-storey braced timber frames, *Canadian Journal of Civil Engineering*, Vol 30(6) 1089-1100.
- Ramirez, C.M. & Miranda, E. 2012. Significance of residual drifts in building earthquake loss estimation. *Earthquake engineering & structural dynamics*, Vol 41(11) 1477-1493.
- Rodgers, G.W., Mander, J.B., Chase, J.G. & Dhakal, R.P. 2015. Beyond ductility: parametric testing of a jointed rocking beam-column connection designed for damage avoidance, *Journal of Structural Engineering*, Vol 142(8), C4015006.
- Vafaei, D. & Eskandari, R. 2015. Seismic response of mega buckling- restrained braces subjected to fling- step and forward- directivity near- fault ground motions, *The Structural Design of Tall and Special Buildings*, Vol 24(9) 672-686.
- Veismoradi, S., Cheraghi, A. & Darvishan, E. 2018. Probabilistic mainshock-aftershock collapse risk assessment of buckling restrained braced frames, *Soil Dynamics and Earthquake Engineering*, Vol 115 205-216.
- Wijanto, S. 2012. *Behaviour and Design of Generic Buckling Restrained Brace Systems*. University of Auckland.
- Yousef-beik, S.M.M., Zarnani, P., Mohammadi, F., Darani, A.H. & Quenneville, P. 2018. New Seismic Damage Avoidance Timber Brace Using Innovative Resilient Slip Friction Joints for Multi-story Application, *World Conference on Timber Engineering, WCTE 2018*, Seoul, Korea.
- Zarnani, P. & Quenneville, P. 2015. *A Resilient Slip Friction Joint*. Patent No.WO2016185432A1, NZ IP Office.
- Zarnani, P., Valadbeigi, A. & Quenneville, P. 2016. Resilient slip friction (RSF) joint: A novel connection system for seismic damage avoidance design og timber structures, *World Conf. on Timber Engineering, WCTE 2014*, Vienna Univ. of Technology, Vienna, Austria.